

## Beat-Wave Resonant Down Scattering of Diocotron and Kelvin Modes

Nathan Mattor, B. T. Chang, and T. B. Mitchell\*

*Department of Physics & Astronomy, University of Delaware, Newark, Delaware 19716, USA*

(Received 13 August 2005; published 31 January 2006)

A theory is presented of beat-wave resonant down scattering of two-dimensional diocotron (or Kelvin) modes, in which modes down scatter to lower azimuthal mode number. The phenomenon is a fluid analogue to nonlinear Landau damping. The principal new result is a quantitative prediction of the scattering rate. The predicted rates and scalings are close to those observed in experiments with magnetized electron columns.

DOI: [10.1103/PhysRevLett.96.045003](https://doi.org/10.1103/PhysRevLett.96.045003)

PACS numbers: 52.27.Jt, 47.32.C-, 52.35.Mw

One embodiment of self-organization is the phenomenon of down scattering. This refers to the evolution of spectral energy from high to low wave number, and can appear as an initially complicated spectrum of fluctuations evolving to a more coherent state. Down scattering has been associated with such diverse phenomena as the appearance of coherent structures in fully developed turbulence [1], generation of atmospheric zonal flows [2], and formation of low numbered spiral density waves in astrophysical disks [3]. Unfortunately down scattering involves fairly difficult nonlinear wave coupling, and dynamical understanding is still emerging.

An experiment described in Ref. [4] generated down scattering in a magnetized pure electron plasma, a system with dynamics closely analogous to a two-dimensional fluid [5,6]. Initializing the plasma with a single  $m = 4$  diocotron mode (analogous to a Kelvin mode on a fluid vortex), it was observed that the mode deforms with time, and then evolves into an  $m = 3$  and then  $m = 2$  and  $m = 1$ . Down scattering was subsequently observed in simulations of the same physical system, with a stretch-split-partial-merger mechanism invoked to explain the phenomena [7].

This Letter describes a theory of down scattering in terms of beat-wave resonance, and shows that the predicted scattering rates are close to those observed. The basic mechanism acts as follows. The initial test wave ( $m, \omega$ ) interacts nonlinearly with a background wave ( $m', \omega'$ ) to form a beat wave at  $(m - m', \omega - \omega')$ . When the background fluid has differential rotation, say angular velocity  $\Omega(r)$ , then there is a particular radius  $r_s$  where the beat wave and the fluid rotate with the same velocity,  $\Omega(r_s) = (\omega - \omega')/(m - m')$ . At  $r_s$  the beat wave resonates with the fluid, in a manner analogous to nonlinear Landau damping in a kinetic plasma. The net effect of this resonance is an energy transfer between the two primary waves  $m$  and  $m'$ . This effect has been examined theoretically in several systems [3,8,9], but apparently none of these have been successfully compared quantitatively with experiment.

The model and equations are as follows. The pure electron plasma is permeated by a straight magnetic field  $\mathbf{B}$ , bounded by a cylindrical conducting wall, and confined at

the ends by an electrostatic potential. We use cylindrical coordinates  $(r, \theta, z)$ , with  $z$  aligned with the magnetic field,  $\hat{\mathbf{z}} = \mathbf{B}/B$ . The basic equations are

$$\frac{\partial}{\partial t} n + \nabla \cdot (n\mathbf{v}) = 0, \quad (1)$$

$$\nabla^2 \phi = 4\pi en, \quad (2)$$

where  $\mathbf{v} = (c/B)\hat{\mathbf{z}} \times \nabla\phi$  is the  $E \times B$  velocity,  $n(r, \theta)$  is the electron density,  $\phi(r, \theta)$  is the electrostatic potential,  $\mathbf{B}$  is the constant magnetic field. The plasma is surrounded by a conducting wall at  $r = R_w$ , giving the boundary condition  $\phi(R_w, \theta) = \text{const}$ . These equations also coincide with the Euler equation for a two-dimensional inviscid fluid [5,6], so our theory applies equally well to the case of a 2D vortex surrounded by a circular free-slip boundary.

The scattering rate is calculated as follows. The fields are divided into the azimuthally averaged components (denoted with subscript 0) and the remainder, so that  $n(r, \theta) = n_0(r) + \tilde{n}(r, \theta)$  and so on. Taking the fluctuating components of Eqs. (1) and (2) and Fourier transforming in  $t$  and  $\theta$  gives

$$L_{\mathbf{p}} \tilde{n}_{\mathbf{p}} = -in'_0 \tilde{v}_{r\mathbf{p}} - i \sum_{\mathbf{p}'} \tilde{\mathbf{v}}_{\mathbf{p}'} \cdot \nabla \tilde{n}_{\mathbf{p}-\mathbf{p}'}, \quad (3)$$

$$\nabla^2 \tilde{\phi}_{\mathbf{p}} = 4\pi e \tilde{n}_{\mathbf{p}}, \quad (4)$$

where  $\tilde{v}_{r\mathbf{p}} \equiv \hat{\mathbf{r}} \cdot \tilde{\mathbf{v}}_{\mathbf{p}}$ ,  $L_{\mathbf{p}} \equiv \omega - m\Omega(r)$ ,  $n'_0 \equiv dn_0/dr$ ,  $m$  and  $\omega$  are the Fourier conjugates of  $\theta$  and  $t$ , the index  $\mathbf{p}$  stands for the vector  $(m, \omega)$ , and the  $\theta$  component of  $\nabla$  applied to Fourier transformed quantities stands for  $i/r$  times the sum of azimuthal mode indices of the terms operated on. The index  $\omega$  is actually continuous, but we denote  $\int d\omega$  informally as a sum for brevity.

Assuming the nonlinearity is small enough to be treated perturbatively, Eqs. (3) and (4) can be addressed with a weak turbulence expansion [10]. Thus expanding  $\tilde{n}_{\mathbf{p}} = \tilde{n}_{\mathbf{p}}^{(1)} + \tilde{n}_{\mathbf{p}}^{(2)} + \tilde{n}_{\mathbf{p}}^{(3)} + \dots$  in successive powers of  $\tilde{\phi}$ , these obey the equations

$$L_{\mathbf{p}}\tilde{n}_{\mathbf{p}}^{(1)} = -in'_0\tilde{v}_{r\mathbf{p}}, \quad L_{\mathbf{p}}\tilde{n}_{\mathbf{p}}^{(2)} = -i\sum_{\mathbf{p}'}\tilde{\mathbf{v}}_{\mathbf{p}'}\cdot\nabla\tilde{n}_{\mathbf{p}-\mathbf{p}'}^{(1)},$$

$$L_{\mathbf{p}}\tilde{n}_{\mathbf{p}}^{(3)} = -i\sum_{\mathbf{p}'}\tilde{\mathbf{v}}_{\mathbf{p}'}\cdot\nabla\tilde{n}_{\mathbf{p}-\mathbf{p}'}^{(2)}.$$

Eliminating the  $n^{(a)}$  in favor of  $\tilde{\phi}$  and  $\tilde{\mathbf{v}}$  (directly related), and substituting into Eq. (4) produces

$$\epsilon_{\mathbf{p}}^{(1)}\tilde{\phi}_{\mathbf{p}} + \sum_{\mathbf{p}'+\mathbf{p}''=\mathbf{p}}\epsilon_{\mathbf{p}',\mathbf{p}''}^{(2)}\tilde{\phi}_{\mathbf{p}'}\tilde{\phi}_{\mathbf{p}''}$$

$$+ \sum_{\mathbf{p}'+\mathbf{p}''=\mathbf{p}}\sum_{\mathbf{p}'''}\epsilon_{\mathbf{p}',\mathbf{p}'',\mathbf{p}'''}^{(3)}\tilde{\phi}_{\mathbf{p}'}\tilde{\phi}_{\mathbf{p}''}\tilde{\phi}_{\mathbf{p}'''} = 0, \quad (5)$$

where the operators  $\epsilon^{(n)}$  are defined by

$$\epsilon_{\mathbf{p}}^{(1)} \equiv L_{\mathbf{p}}\nabla^2 + \frac{4\pi ecn'_0}{B}\frac{m}{r},$$

$$\epsilon_{\mathbf{p}',\mathbf{p}''}^{(2)}\tilde{\phi}_{\mathbf{p}'}\tilde{\phi}_{\mathbf{p}''} \equiv 4\pi e\nabla\cdot\left[\frac{n'_0\tilde{\mathbf{v}}_{\mathbf{p}'}\tilde{v}_{r\mathbf{p}''}}{L_{\mathbf{p}}-L_{\mathbf{p}'}}\right],$$

$$\epsilon_{\mathbf{p}',\mathbf{p}'',\mathbf{p}'''}^{(3)}\tilde{\phi}_{\mathbf{p}'}\tilde{\phi}_{\mathbf{p}''}\tilde{\phi}_{\mathbf{p}'''} \equiv -4\pi e i\nabla\cdot\left[\frac{\tilde{\mathbf{v}}_{\mathbf{p}'}\tilde{\mathbf{v}}_{\mathbf{p}''}}{L_{\mathbf{p}}-L_{\mathbf{p}'}}\cdot\nabla\left[\frac{n'_0\tilde{v}_{r\mathbf{p}''}}{L_{\mathbf{p}''}}\right]\right].$$

To lowest order, Eq. (5) describes linear normal modes (diocotron or Kelvin modes). Taking the lowest order solution as  $\tilde{\phi}_{\mathbf{p}} \simeq \tilde{\phi}_{\mathbf{p}}^{(1)}$ , the lowest order equation is  $\epsilon_{\mathbf{p}}^{(1)}(r)\tilde{\phi}_{\mathbf{p}}^{(1)}(r) = 0$ , which is the well-known Rayleigh stability equation in cylindrical geometry [11]. The boundary condition is  $\tilde{\phi}_{\mathbf{p}}(a) = 0$  for  $m \neq 0$ , which gives  $\phi^{(1)}$  as a spectrum of normal modes with real eigenfrequency  $\omega_{\mathbf{k}}$

$$\tilde{\phi}_{\mathbf{p}}^{(1)}(r) = \sum_n \hat{\phi}_{\mathbf{k},\omega}(r) = \sum_n \hat{\phi}_{\mathbf{k}}(r)\delta(\omega - \omega_{\mathbf{k}}), \quad (6)$$

where  $n$  is a radial mode index, and the subscript  $(\ )_{\mathbf{k}}$  is short for  $(\ )_{m,n}$ . Orthogonal eigenmodes are obtained from the adjoint operator,  $\epsilon_{\mathbf{p}}^{(1)\dagger}$ , defined by exchanging  $\nabla^2$  and  $L_{\mathbf{p}}$  in  $\epsilon_{\mathbf{p}}^{(1)}$ . The eigenmodes of  $\epsilon_{\mathbf{p}}^{(1)\dagger}$  are given by  $\hat{\phi}_{\mathbf{k}}^\dagger = \hat{\phi}_{\mathbf{k}}/L_{\mathbf{k}}$ , where  $L_{\mathbf{k}} \equiv \omega_{\mathbf{k}} - m\Omega$ . It can be readily shown that  $\hat{\phi}_{\mathbf{k}}^\dagger$  and  $\hat{\phi}_{\mathbf{k}}$  are orthogonal in the sense that  $\int_0^a r dr \nabla \hat{\phi}_{m,n}^{\dagger*} \cdot \nabla \hat{\phi}_{m,n'} \propto \delta_{n,n'}$ , where  $\delta_{n,n'}$  is the Kronecker  $\delta$  function and  $\hat{\phi}_{-m,-n} = \hat{\phi}_{m,n}^*$ . Other linear properties are described in Refs. [11,12].

The evolution of wave amplitude is described by the wave kinetic equation. This is obtained by applying the annihilation operator  $\text{Im} \int_0^a r dr \int d\omega e^{-i\omega t} \hat{\phi}_{\mathbf{k}}^{\dagger*}(r, t)$  to Eq. (5). We assume the  $m = 0$  component is stationary on the time scale of the  $m > 0$  amplitude evolution, which allows the radial dependence of the eigenmodes to be treated as fixed [13]. The  $\epsilon^{(2)}$  term gives shielding and 3-wave resonances [10,12]. The former can be shown to give no contribution to beat-wave resonance. The latter occurs only when there are 3-wave frequency matches,  $\omega_{\mathbf{k}} = \omega_{\mathbf{k}'} + \omega_{\mathbf{k}-\mathbf{k}'}$ ; we assume none, and drop  $\epsilon^{(2)}$ . This gives

$$\frac{1}{2}\frac{\partial}{\partial t}\int_0^a r dr \text{Re}[\hat{\phi}_{\mathbf{k}}^{\dagger*}\hat{n}_{\mathbf{k}}]$$

$$+ \text{Im} \sum_{\mathbf{p}'+\mathbf{p}''=\mathbf{p}} \sum_{\mathbf{p}'''} \int_0^a r dr \int d\omega e^{-i\omega t} i\nabla \hat{\phi}_{\mathbf{k}}^{\dagger*}$$

$$\cdot \frac{\tilde{\mathbf{v}}_{\mathbf{p}'}\tilde{\mathbf{v}}_{\mathbf{p}''}}{L_{\mathbf{p}}-L_{\mathbf{p}'}} \cdot \nabla \left[ \frac{n'_0\tilde{v}_{r\mathbf{p}''}}{L_{\mathbf{p}''}} \right] = 0, \quad (7)$$

where  $4\pi e\hat{n}_{\mathbf{k}} = \nabla^2 \hat{\phi}_{\mathbf{k}}$ . Using Eq. (6) for the lowest order contribution to the various  $\tilde{v}_{\mathbf{p}}$  in the nonlinear term and averaging over the assumed rapid oscillations produces a delta function  $\delta(\omega_{\mathbf{k}} - \omega_{\mathbf{k}'} - \omega_{\mathbf{k}''} - \omega_{\mathbf{k}'''})$ . Assuming the only frequency matches are those from the reality constraint leaves contributions from  $\mathbf{k}'' = -\mathbf{k}'$  and  $\mathbf{k}'' = \mathbf{k}$ . After some manipulation this gives

$$\frac{1}{2}\frac{\partial}{\partial t}\int_0^a r dr \text{Re}[\hat{\phi}_{\mathbf{k}}^{\dagger*}\hat{n}_{\mathbf{k}}] + \text{Im} \sum_{\mathbf{k}'} \int_0^a r dr \hat{\mathbf{v}}_{\mathbf{k}'} \cdot \nabla \hat{\phi}_{\mathbf{k}}^{\dagger*}\hat{\mathbf{v}}_{\mathbf{k}'}$$

$$\cdot \left[ \frac{n'_0 c m'' L_{\mathbf{k}}}{r B L_{\mathbf{k}'} L_{\mathbf{k}''}} \nabla \hat{\phi}_{\mathbf{k}}^\dagger + \nabla \left( \frac{\hat{n}_{\mathbf{k}}}{L_{\mathbf{k}'}} \right) \right] = 0, \quad (8)$$

where  $L_{\mathbf{k}''} \equiv L_{\mathbf{k}} - L_{\mathbf{k}'}$  and  $m'' \equiv m - m'$ . The propagator  $L_{\mathbf{k}''}^{-1}$  has two parts: a principal value and a resonance. We evaluate these via the Landau bypass rule [14]

$$\frac{1}{\omega'' - m''\Omega(r)} \simeq \text{P.V.} - \frac{\pi i}{|m''\Omega'(r_s)|} \delta(r - r_s), \quad (9)$$

where P.V. stands for the principal value,  $r_s$  is the radius where  $\omega'' - m''\Omega(r_s) = 0$ , and  $\Omega' \equiv d\Omega/dr$ . The P.V. part of the integral and the resonances from  $L_{\mathbf{k}}^{-1}$  and  $L_{\mathbf{k}'}^{-1}$  give small nonlinear corrections to linear terms, and do not contribute to scattering. We neglect them here for brevity.

Applying Eq. (9) to  $L_{\mathbf{k}''}$  in Eq. (8), and keeping only the resonance gives the wave kinetic equation in remarkably simple form

$$\frac{1}{2}\frac{\partial}{\partial t}\int_0^a dr \frac{mr^2|\hat{n}_{\mathbf{k}}|^2}{n'_0} = - \sum_{\mathbf{k}'} \frac{\pi n'_0 m''}{|m''\Omega'|} \left| \hat{\mathbf{v}}_{\mathbf{k}'} \cdot \nabla \left( \frac{\hat{\phi}_{\mathbf{k}}}{L_{\mathbf{k}}} \right) \right|^2 \Big|_{r=r_s}. \quad (10)$$

Equation (10) is the main result of this derivation. The left side represents the evolution of wave action, and the right side the nonlinear scattering interaction. Scattering conserves wave action, since the right side vanishes when summed over all modes. The sign of the scattering rate is determined by  $n'_0$ , negative here, and  $m'' = m - m'$ . This results in action lost by higher  $m$  and absorbed by lower  $m$ : down scattering. Physically, the scattering involves  $\hat{\mathbf{v}}_{\mathbf{k}'}$  convecting the contours of  $\hat{\phi}_{\mathbf{k}}/L_{\mathbf{k}}$  at  $r_s$ . The function  $\hat{\phi}_{\mathbf{k}}/L_{\mathbf{k}}$  can be interpreted as a generating function for the Lagrangian displacement [15], which implies that there may be a very simple Lagrangian derivation of Eq. (10).

The derivation neglects several effects. *Trapping*, in which the density flattens in the region of the resonance and reduces the effects of a resonance [16,17], is negligible here. Estimates show that the fluid orbit rate in the beat wave is about 2 orders of magnitude slower than the

decorrelation rate of the beat wave due to differential propagation of  $\hat{\phi}_{\mathbf{k}}$  and  $\hat{\phi}_{\mathbf{k}'}$ . Experimentally, ten consecutive cycles of parent mode growth and decay damping are found to be needed to produce significant levels of density transport and down scattering rate change. *Shielding* can with effort be shown to give no contribution to the beat-wave resonance. *Three-wave resonances* were not observed in the experiments, since there were no three-way frequency matches. Other density profiles may exist which *do* have such matches [18]. A two-time scale expansion, necessary to avoid secular terms in a full analysis [12], involves much more effort than shown here but gives the same result for the terms considered here. Evolution of the  $m = 0$  component can also give terms in the wave kinetic equation, but we have neglected it under the experimentally justified assumption that the wave amplitude evolves on a much faster scale.

It is straightforward to apply the 2D theory to 3D experimental measurements. A schematic of the experimental apparatus used is shown in Fig. 1. A column of electrons of temperature  $T \simeq 2$  eV is confined inside a series of conducting rings of wall radius  $R_w = 2.88$  cm and confinement length  $L_c = 36.0$  cm, in a uniform axial magnetic field  $B_z = 454$  Ga. The magnetic field provides radial confinement, and negative confinement voltages of  $V_c = -75$  V applied to end gate rings provide axial confinement. The rapid axial bounce motion of individual electrons effectively averages over the  $z$  variations, allowing a 2D description of the system. The  $r, \theta$  flow of the electrons is thus well described by the 2D drift Poisson equations, Eqs. (1) and (2). The vorticity of the flow,  $\zeta \equiv \hat{z} \cdot \nabla \times \mathbf{v} = \frac{4\pi ec}{B} n = 0.399n$ , is proportional to the electron density, which is directly measured in the experiment.

In the measurements, an electron column is injected and trapped, then shaped and azimuthally symmetrized using wall sectors. A single diocotron mode with chosen azimuthal mode number  $m$  and  $k_z = 0$  is then grown to the desired amplitude, while all other modes are damped with negative feedback. All feedback is then turned off, and the subsequent evolution of the various modes is monitored with a spectrum analyzer. Parent mode initial amplitude  $A_m$  and the daughter mode growth rate  $\gamma_{m-1}$  can be obtained from a single evolution in this fashion. To study the mode evolution or to calibrate the mode amplitude with the measured signal amplitudes, the electron column can be dumped axially, and images made of the electron line charge number distribution  $N(r, \theta)$  which strikes a phosphor screen biased to 5.5 kV.

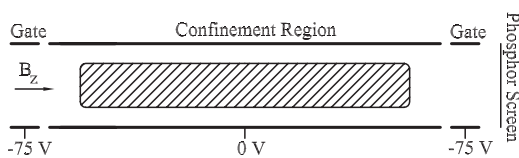


FIG. 1. Schematic of the cylindrical electron plasma confinement geometry.

In order to compare the 3D experiment with the 2D theory, we calculate an equivalent axisymmetric 2D density profile  $n_0(r)$  from the measurement of  $N(r, \theta)$ . This is divided into an azimuthally averaged component and the remainder, so that  $N(r, \theta) = N_0(r) + \tilde{N}(r, \theta)$ . The axisymmetric 3D density  $n(r, z)$  and electric potential  $\phi(r, z)$  are then determined by iteratively solving Poisson's equation with the constraint  $N_0(r) = \int dz n(r, z)$  and the assumption that the electrons are well described by a local Boltzmann distribution along each magnetic field line [19]. The boundary conditions are set by the gate voltages  $V_c$  and the confinement length  $L_c$ . From the potentials we calculate the  $\theta$  drifts caused by the radial component of the electric field given by  $v_\theta(r, z) = \frac{c}{B} E_r(r, z)$ .

We remove the  $z$  dependence of quantities by using a density-weighted average. For example, the azimuthally averaged 2D electron density  $n_0(r)$  is given by  $n_0(r) \equiv \frac{1}{N_0(r)} \int dz n(r, z) n(r, z)$ . This quantity and the 2D rotation frequency  $\Omega(r)$  are plotted in Fig. 2 for a typical column with a low-amplitude  $m = 3$  mode (also shown).

Finite-length effects exist, although they are relatively small. For example, there are  $\theta$  drifts from the radial components of the confining electric fields at the ends [20]. The density-weighted confinement frequency shift from these is additive, and varies from 11.6 kHz on the axis to 7.5 kHz on the edge of the column. The ends of the column are also not exactly flat, but defining the radially dependent plasma length as  $L(r) \equiv N_0(r)/n_0(r)$ , the variation in length is less than 4% across the radius of the column.

We use the column length to calculate the equivalent 2D Fourier mode amplitudes through  $\hat{n}_{\mathbf{k}}(r) \equiv \hat{N}_{\mathbf{k}}(r)/L(r)$ . In general, we see good agreement between the observed eigenfunctions  $\hat{n}_{\mathbf{k}}$  and eigenfrequencies, and those predicted for an infinitely long cylinder with the same density profile  $n_0$ . We determine the solutions of  $\epsilon_{\mathbf{p}}^{(1)} \tilde{\phi}_{\mathbf{p}}^{(1)} = 0$  using a matrix shooting code [21]. In Fig. 2 we plot its prediction for the  $m = 3$  eigenfunction (dotted line).

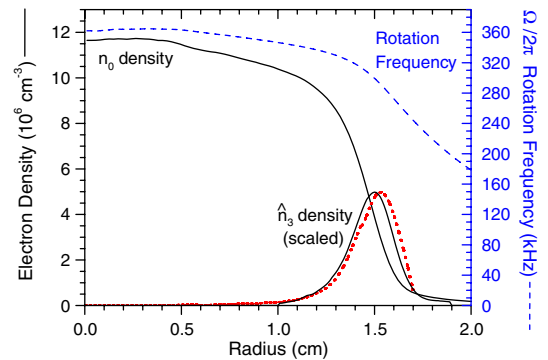


FIG. 2 (color online). Calculated density profile  $n_0$  and  $m = 3$  eigenfunction (lines) and rotation frequency  $\Omega(r)/2\pi$  (dashed line) for the case of a low-amplitude  $m = 3$  mode. A calculated 2D  $m = 3$  mode eigenfunction (dotted line) is also plotted.

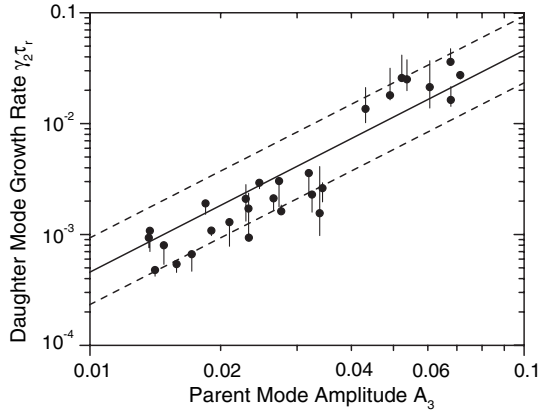


FIG. 3. Measured (line) and predicted (symbols)  $m = 2$  daughter mode growth rates.

In order to evaluate the scattering rates, we rewrite Eq. (10) in a form where potentials have been eliminated, and assume the amplitude but not the shape of  $\hat{v}_{\mathbf{k}}$  varies in time. With a definition of wave action  $J_{\mathbf{k}} \equiv \int_0^a r^2 dr m |\hat{n}_{\mathbf{k}}|^2 / n_0'$ , the growth rate  $\gamma_{\mathbf{k}}$  of a daughter mode  $\mathbf{k}$  in the presence of a parent mode  $\mathbf{k}'$  is

$$\gamma_{\mathbf{k}} = \frac{-1}{J_{\mathbf{k}}} \sum_{\mathbf{k}'} \frac{\pi n_0' m''}{|m'' \Omega'|} \left| \hat{v}_{\mathbf{k}'}^* \cdot \nabla \left( \frac{r \hat{n}_{\mathbf{k}}}{n_0'} \right) \right|^2 \Big|_{r=r_s}. \quad (11)$$

For the case of the measured  $n_0$  density profile and mode eigenfunction shown in Figs. 2, Fig. 3 shows predicted  $m = 2$  daughter mode growth rates  $\gamma_2$  as a function of the  $m = 3$  parent mode amplitude  $A_3$  (solid line). Mode amplitude is defined by  $A_k \equiv \int_0^{R_w} 2 |\hat{n}_k(r)| r dr / \int_0^{R_w} n_0(r) r dr$ , where the factor of 2 arises from our Fourier transform convention  $2 \hat{n}_k = \delta n_k$ . The growth rates are scaled by the central rotation time  $\tau_r \equiv 2\pi / \Omega(0)$ . The  $\gamma_2$  rates are extremely sensitive to the position of  $r_s$  and to the shape of  $n_0$  and the eigenfunctions. We estimate that, given our ability to control the initial condition only to within 1% in density, a spread in predicted down scatter rates of a factor of 2 is indicated. We indicate this estimated range for rates with dashed lines. The symbols are experimental measurements of  $\gamma_2$ , with error bars indicating measurement uncertainty. Consistent with the theory prediction here of a sensitive dependence on initial conditions, we find that identically prepared electron columns exhibit growth rates with a fairly large scatter.

We have made several such comparisons between the predictions of Eq. (10) and both new experimental measurements and those presented in Ref. [4]. The set of measured scattering rates spans 4 orders of magnitude. In general, we find good agreement with the predicted  $A_k^2$  scaling of mode amplitude, and quantitative agreement with the predicted scattering rates at the 50% level or better. Other predictions of the 2D theory, such as the location of resonance points and sensitivity to initial conditions, also match the experimental observations well. This is the first successful quantitative theory for this

down scattering phenomena, and the agreement lends credence to a similar theory for astrophysical disks [3].

In future work, it would be useful to connect our very specific beat-wave down scattering with some more general theory, such as entropy minimization often associated with self-organization. The awkward derivation of Eq. (10) could be greatly simplified with a Lagrangian approach in the style of Ref. [15]. Numerical simulation could extend the understanding gained here to regimes where the theory breaks down. Of the neglected effects, probably large amplitude and trapping effects are the most important.

This work was supported by National Science Foundation Grant No. PHY-0140318, University of Delaware Research Foundation Grant No. LTR20010426, and U.S. Department of Energy Grant No. DE-FG02-06ER54853. The authors thank R.L. Spencer for software analysis contributions and Erin Burkett for experimental contributions.

\*Electronic address: tbmitche@udel.edu

- [1] C. E. Leith, *Phys. Fluids* **27**, 1388 (1984).
- [2] P. B. Rhines, *Annu. Rev. Fluid Mech.* **18**, 433 (1986).
- [3] N. Mattor and T. B. Mitchell, *Astrophys. J.* **472**, 532 (1996).
- [4] T. B. Mitchell and C. F. Driscoll, *Phys. Rev. Lett.* **73**, 2196 (1994).
- [5] R. H. Levy, *Phys. Fluids* **8**, 1288 (1965).
- [6] C. F. Driscoll and K. S. Fine, *Phys. Fluids B* **2**, 1359 (1990).
- [7] H. B. Yao and N. J. Zabusky, *Phys. Fluids* **8**, 1842 (1996).
- [8] L. D. Landau and E. M. Lifshitz, *Fluid Mechanics* (Pergamon Press, Oxford, 1987).
- [9] J. D. Crawford and T. M. O'Neil, *Phys. Fluids* **30**, 2076 (1987).
- [10] R. Z. Sagdeev and A. A. Galeev, *Nonlinear Plasma Theory* (Benjamin, New York, 1969).
- [11] P. G. Drazin and W. H. Reid, *Hydrodynamic Stability* (Cambridge University Press, Cambridge, England, 1981).
- [12] R. C. Davidson, *Physics of Nonneutral Plasmas* (Addison-Wesley Publishing, New York, 1990).
- [13] The approach used here entails the heuristic assumption that  $\tilde{\phi}_{\mathbf{k}}^{(1)}$  acquires time dependence at next order. A more formal analysis requires a multiple time-scale analysis (see Davidson, Ref. [12]), skipped here for expediency.
- [14] V. V. Timofeev, *Reviews of Plasma Physics 17* (Consultants Bureau, New York, 1992).
- [15] A. J. Brizard, *Phys. Plasmas* **3**, 744 (1996).
- [16] T. M. O'Neil, *Phys. Fluids* **10**, 1027 (1967).
- [17] T. Warn and H. Warn, *Stud. Appl. Math.* **59**, 37 (1978).
- [18] L. Friedland and A. G. Shagalov, *Phys. Fluids* **14**, 3074 (2002).
- [19] R. L. Spencer, S. N. Rasband, and R. R. Vanfleet, *Phys. Fluids B* **5**, 4267 (1993).
- [20] K. S. Fine and C. F. Driscoll, *Phys. Plasmas* **5**, 601 (1998).
- [21] G. W. Mason and R. L. Spencer, *Phys. Plasmas* **9**, 3217 (2002).